

A three-dimensional tetrahedral-shaped conjugated small molecule for organic solar cells

QIN Yang, YANG Jianzhong

(Department of Chemistry & Chemical Biology, University of New Mexico, Albuquerque NM 87131-001, U. S. A.)

Abstract: We report the synthesis of a novel three-dimensional tetrahedral-shaped small molecule, **SO**, containing a tetraphenylsilane core and cyanoester functionalized terthiophene arms. A deep lying HOMO energy level of -5.3 eV and a narrow bandgap of 1.9 eV were obtained from cyclic voltammetry measurements. Absorption, X-ray scattering and differential scanning calorimetry experiments all indicate high crystallinity of this compound. Solar cells employing **SO** were fabricated and evaluated. The relatively low performance was mainly ascribed to lack of appreciable phase separation, which is confirmed by optical microscopy.

Key words: tetrahedral-shaped small molecule; organic solar cell; crystallinity; phase separation

CLC number: TM 914.4 **Document code:** A **Article ID:** 1000-5137(2014)02-0159-09

1 Introduction

Organic solar cells have attracted tremendous attention from both academia and industry due to the promises as low-cost alternative energy sources^[1-2]. Research efforts in these areas have mostly been devoted to materials based on conjugated polymers^[3-5], and power conversion efficiencies (PCEs) of these devices have steadily increased to approach 10% in laboratory settings^[6-8]. However, the intrinsic polydisperse and amorphous nature of conjugated polymers often leads to batch-to-batch variations and low materials conductivity, respectively, which can potentially impede device mass production and further improvement. On the other hand, conjugated small molecules can be highly crystalline, while having discrete and reproducible molecular structures^[7-11]. Bulk heterojunction (BHJ) devices employing conjugated small molecules and fullerene derivatives have been constantly improved to rival their conjugated polymer counterparts and thus shown great promises in solar cell research^[12-14].

Most small molecules applied in solar cells have linear structures containing multiple aromatic groups connected in series. Such molecules are typically highly crystalline and conductive along the π -stacking direction. However, charge migration along both long and short axes are relatively limited due to the one-dimensional nature of these molecules. Unfavorable film forming ability and grain boundaries originated from high crystallinity of linear molecules can also have detrimental effects on device performances. Thus, small molecules having conjugation extended in three-dimensions (3-D) can offer both good film forming ability and isotropic charge mobility. Tet-

Received date: 2014-03-26

Foundation item: National Science Foundation (NSF) is unacknowledged for supporting the NMR facility at UNM through grants CHE-0840523 and 0946690.

Biography: QIN Yang, male, assistant professor.

Corresponding author: QIN Yang, E-mail: yangqin@unm.edu

ra-substituted silanes have been a common starting core for building 3-D molecules due to the tetrahedral geometry and easy preparation. Roncali etc. reported the synthesis of two silane-cored terthiophene armed 3-D small molecules bearing respective alkyl and thioalkyl side chains^[15]. Although overall solar cell performances were significantly limited by narrow absorption due to the large bandgaps, both star-shaped molecules outperformed their corresponding single-arm counterparts, proving the effectiveness of 3-D strategy. Köse etc. recently reported low bandgap small molecules based on tetrathienyl core and benzothiadiazole containing arms and found favorable impact of high dimensionality on charge mobility in disordered media^[16]. On the other hand, silicon thio-phenone bonds are quite unstable due to the electron richness of thienyl moieties, which can potentially complicate synthesis and reduce device lifetimes. Herein, we report the synthesis and characterization of a stable low bandgap 3-D conjugated molecule based on tetraphenylsilane core. Initial investigation of this molecule in BHJ solar cells indicates that lack of phase separation with fullerene molecules is responsible for relatively low device performance.

2 Results and discussions

Synthesis of the 3-D conjugated small molecule **SO** is shown in Figure 1 and synthetic details can be found in the experimental section. The compound **1** was prepared from commercial 1,4-dibromobenzene through lithium halogen exchange followed by reaction with SiCl_4 , which can be conveniently used as a common core for grafting with different arms toward 3-D molecules. After Stille coupling reaction with **10** followed by acetal deprotection, the tetra-aldehyde compound **11** was obtained. The aldehyde groups can be transformed to several strongly electron withdrawing substituents, e. g. dicyanovinyl and cyanoester groups. However **11** was found to have very limited solubility in common organic solar cell processing solvents such as chlorobenzene and dichlorobenzene. We thus chose *n*-octyl cyanoacetate (**12**) to install the functionality. Indeed, after a simple condensation reaction, compound **SO** was obtained in high yields and has good solubility in a wide range of organic solvents including CHCl_3 , THF and chlorobenzene. All compounds are fully characterized by ^1H and ^{13}C NMR spectroscopy, which agree well with proposed structures. High resolution mass spectrometry (HR-MS) was applied to confirm the tetra-arm nature of our target compounds. Unfortunately **SO** could not be ionized under experimental conditions and no meaningful mass signals could be observed. Instead, HR-MS was performed on the precursor **11**, in which the measured molar mass ($1768.3419 [\text{M}^+]$) matches very well with the calculated value ($1768.3414 [\text{M}^+]$), confirming the tetra-arm structure. Since NMR showed full conversion of the aldehyde groups to cyanoester moieties, the compound **SO** unambiguously has the proposed tetra-arm 3-D structure.

The electronic properties of **SO** were first investigated by UV-Vis absorption spectroscopy in both diluted solutions and as thin films as shown in Figure 2. A structureless absorption profile with a $\lambda_{\text{max}} = 478 \text{ nm}$ was observed in solution, originated from intra-molecular charge transfer interactions. From the absorption onset at ca. 560 nm, a solution optical bandgap of ca. 2.2 eV is calculated. Significant red-shift of λ_{max} to 575 nm was observed in the thin film of **SO** and the absorption profile became more structured, indicating aggregation and enhanced crystallinity in the solid state. From the absorption onset at ca. 650 nm, the solid-state bandgap of **SO** is estimated to be ca. 1.9 eV that is comparable to that of the most commonly applied conjugated polymer, poly(3-hexylthiophene) (P3HT). In order to further quantify the frontier energy levels, cyclic voltammetry (CV) measurements were performed on **SO** thin films drop cast onto the glassy carbon working electrode. A Ag/AgCl reference and a Pt wire counter electrodes were used, and 0.1 mol/L tetrabutylammonium hexafluorophosphate in acetonitrile was used as the supporting electrolytes. Two quasi-reversible oxidation peaks at 0.9 V and 1.3 V and one irreversible reduction peak at -1.0 V (all values are onsets) were observed. When calibrated

externally with ferrocene redox couple (-4.8 eV below vacuum $\rho. 4$ V vs. Ag/AgCl), a HOMO energy level of -5.3 eV and a LUMO energy level of -3.4 eV were calculated. This leads to an electrochemical bandgap of 1.9 eV, agreeing very well with the film's optical bandgap.

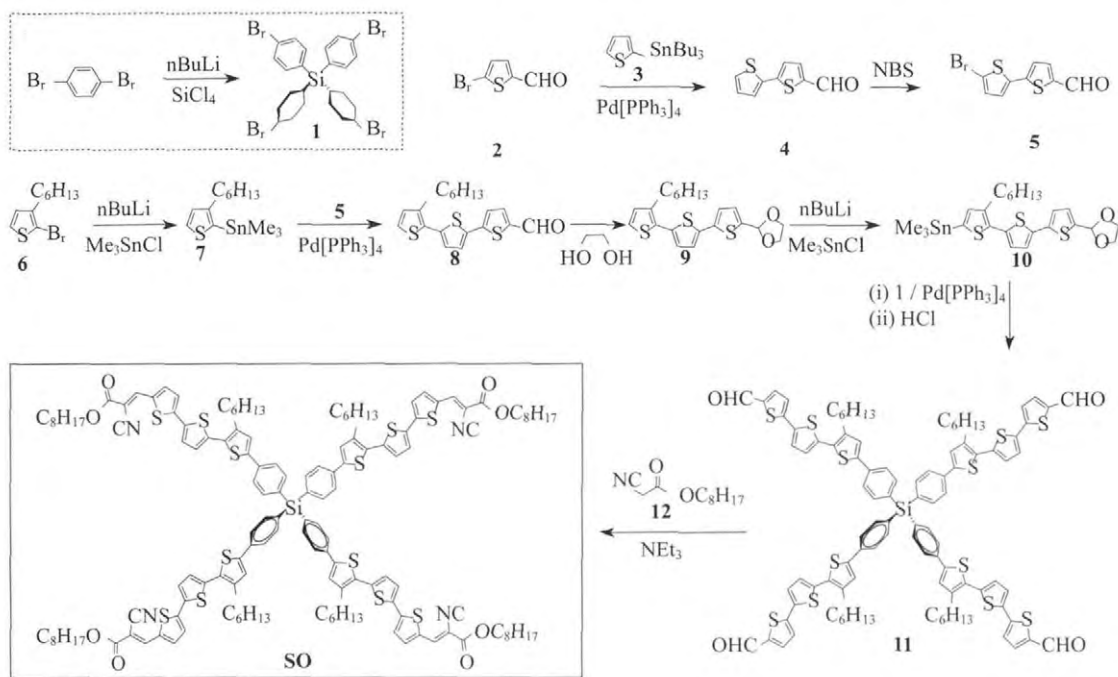


Figure 1 Synthesis of the compound **SO**

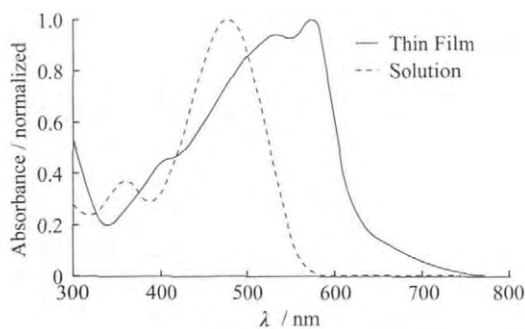


Figure 2 UV-Vis absorption spectra of **SO** in diluted chlorobenzene solution (10^{-5} mol/L, dashed line) and as thin film drop cast onto glass substrate

The absorption spectra indicate certain crystallinity of **SO**, which was further studied by thin film X-ray scattering and differential scanning calorimetry (DSC) measurements. As shown in Figure 3A, the out-of-plane scattering profile clearly contains four distinct peaks at 2θ values of 3.9° , 5.6° , 8.1° and 12.2° , corresponding to d-spacings of 2.3 , 1.6 , 1.1 and 0.7 nm, respectively. Due to the film's small thickness, the signal-to-noise ratio of scattering profiles is not high enough to unambiguously assign the nature of each of these peaks. More detailed studies will be performed on high-power synchrotron sources and the results will be reported in due courses. Crystallinity of **SO** was further confirmed by DSC studies (Figure 3B). The 2nd heating curve showed a glass transition with an onset of 43 °C and a crystallization event peaked at 114 °C. Two closely spaced melting transitions peaked at 180 °C and 187 °C were detected. These observations confirm crystallinity of the **SO** compound.

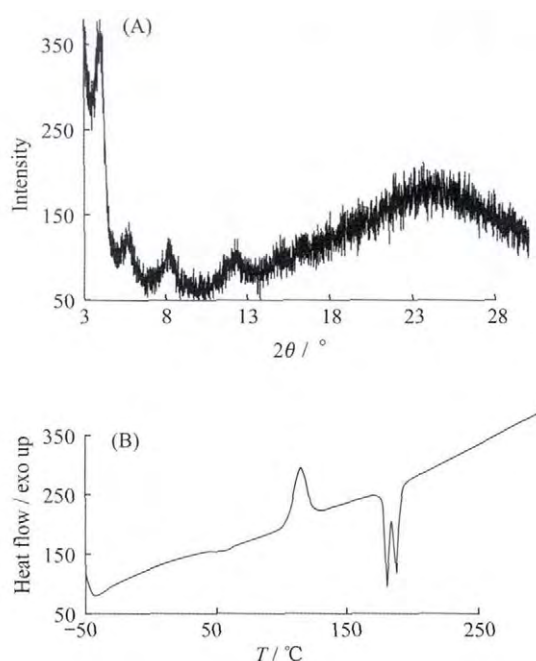


Figure 3 Out-of-plane X-ray scattering profiles of **SO** thin film drop cast on glass substrate (A) and differential scanning calorimetry (DSC) histogram of **SO** powder (2nd heating $10^\circ\text{C}/\text{min}$) (B)

Solar cell devices were fabricated using conventional structures: ITO glass/ MoO_3 (10 nm)/active layer (100 nm)/Al(100 nm). Mixtures of **SO** and phenyl-C61-butyrac methyl ester (PCBM) at various weight ratios in chlorobenzene were spun cast to form the active layer. Thermal annealing at various temperatures was found to deteriorate device performance and the best power conversion efficiencies (PCEs) were found in as cast devices employing **SO**/PCBM at a weight ratio of 1/3. Figure 4 shows the current density-voltage ($I-V$) curves of the best performing device both in dark and under simulated sunlight ($100\text{ mW}/\text{cm}^2$). From the graph an open circuit voltage (V_{oc}) of 0.85 V and a short circuit current (J_{sc}) of $1.1\text{ mA}/\text{cm}^2$ were found and the fill factor (FF) is calculated to be 25%. Device performances suffer greatly from the low FFs and J_{sc} 's. Large current at negative bias was observed in all devices indicating severe geminate charge recombination commonly caused by lack of proper phase separation. We have thus performed optical microscopy measurements on thin films of **SO** and its corresponding blends with PCBM at a 1/3 weight ratio. As shown in Figure 5 optical micrograph of **SO** thin film shows weak crystalline domains (darker areas, A) which becomes significantly enhanced after thermal annealing at 150°C for 10 min (B). This observation is consistent with high crystallinity of the compound. On the other hand both as cast and thermally annealed thin films of **SO**/PCBM blends (1/3 by weight) showed no macroscopic phase separation despite the large excess of PCBM molecules. Certain type of inter-molecular forces between **SO** and PCBM molecules are strong enough to prevent phase segregation the nature of which is currently under investigation.

3 Conclusions

We have successfully prepared a tetraphenylsilane cored 3-D small molecule possessing high crystallinity and low bandgap. Solar cell devices employing such molecule showed lackluster performance due to absence of appreciable phase separation. We are currently optimizing solar cell devices through solvent additives and molecular structural variation in order to gain further insight on the nature of strong interactions of such 3-D mol-

ecules with fullerene acceptors.

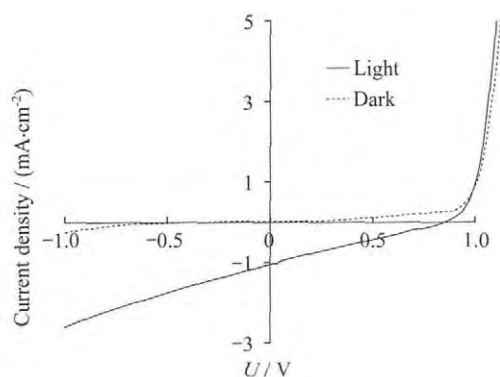


Figure 4 I-V curves of solar cell device employing **SO** and PCBM at a 1/3 weight ratio as the active layer in dark (dashed line) and under simulated white light (100 mW/cm^2)

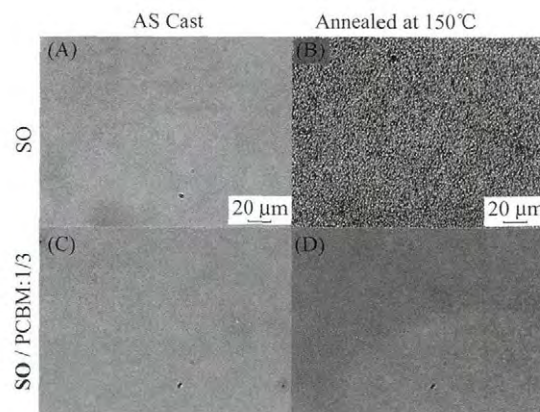


Figure 5 Optical microscopy images (40X zoom) of as cast thin film of **SO** (A) and **SO/PCBM** 1/3 blends (C) and thermally annealed ($150 \text{ }^\circ\text{C}$, 10 min) thin films of **SO** (B) and **SO/PCBM** 1/3 blends (D) (Scale bar: $20 \text{ }\mu\text{m}$)

4 Experimental section

Materials and General Methods All reagents and solvents were used as received from Sigma-Aldrich or Alfa Aesar unless otherwise noted. THF was distilled from Na/benzophenone prior to use. $300.13 \text{ MHz}^1\text{H}$ and $75.48 \text{ MHz}^{13}\text{C}$ NMR spectra were recorded on a Bruker Avance III Solution 300 spectrometer. 2-Tributylstannylthiophene (**3**)^[17], 2,2'-bithiophene-5-carbaldehyde (**4**)^[18], 5'-bromo-(2,2'-bithiophene)-5-carbaldehyde (**5**)^[18], 2-bromo-3-hexylthiophene (**6**)^[19], 3-hexyl-2-trimethylstannylthiophene (**7**)^[20], were prepared to literature procedures. All solution ^1H and ^{13}C NMR spectra were referenced internally to solvent signals. Ultra-violet-Visible (UV-Vis) absorption spectra were recorded on a Shimadzu UV-2401 PC spectrometer over a wavelength range of 240–1100 nm. Fluorescence emission spectra were obtained using a Varian Cary Eclipse fluorimeter. Time-of-flight mass spectrometry (TOF MS) was performed on a Waters/Micromass LCT Premier system operating under atmospheric pressure photoionization (APPI+) mode. Cyclic voltammetry was performed at $25 \text{ }^\circ\text{C}$ on a CH Instrument CHI604xD electrochemical analyzer using a glassy carbon working electrode, a platinum wire counter electrode, and a Ag/AgCl reference electrode calibrated using ferrocene redox couple (4.8 eV below vacuum).

Solar Cell Fabrication and Testing Solar cell devices adopt a structure of ITO/MoO₃/active layer/Al. Thin films of active layers were spin-cast from blend solutions prepared by dissolving **SO** and PCBM (American Dye Source, Inc.) at predetermined weight ratios in chlorobenzene (CB) and stirred at $80 \text{ }^\circ\text{C}$ for 10 h in a nitrogen glove box (Innovative Technology, model PL-He-2 GB, $\text{O}_2 < 10^{-7}$, $\text{H}_2\text{O} < 10^{-7}$) before device fabrication. Solar cell devices were fabricated according to the following procedure: ITO-coated glass substrates (China Shenzhen Southern Glass Display, Ltd) were cleaned by ultrasonication sequentially in detergent, DI water, acetone and isopropyl alcohol, each for 15 min. These ITO-coated glass substrates were further treated by UV-ozone (PSD Series, Novascan) for 45 min before transferred into a nitrogen glove box (Innovative Technology, model PL-He-4GB-1800, $\text{O}_2 < 10^{-7}$, $\text{H}_2\text{O} < 10^{-7}$) for MoO₃ deposition. MoO₃ (10 nm) was deposited using an Angstrom Engineering Åmod deposition system at a base vacuum level $< 7 \times 10^{-8}$ Torr. The blend solution was first filtered through a $0.45 \text{ }\mu\text{m}$ PTFE filter and spin-coated on top of the MoO₃ layer at preset

speeds for 30 s. Typical thickness of organic layers was ca. 100 nm. Al(100 nm) was finally thermally evaporated through patterned shadow masks as anodes. Current-voltage ($I-V$) characteristics were measured by a Keithley 2400 source-measuring unit under simulated AM1.5 G irradiation ($100 \text{ mW}/\text{cm}^2$) generated by a Xe arc-lamp based Newport 67005 150-W solar simulator equipped with an AM1.5 G filter. The light intensity was calibrated by a Newport thermopile detector (model 818P-010-12) equipped with a Newport 1916-C Optical Power Meter.

Tetrakis(4-bromophenyl) silane (1) 4-Dibromobenzene (5.00 g, 21.2 mmol) was weighed into a dry 100 mL Schlenk flask and 50 mL anhydrous THF was added through cannular. The flask was cooled to -78°C and 8.1 mL $n\text{-BuLi}$ (2.5 mol/L in THF, 20.2 mmol) solution was added dropwise. The reaction mixture was stirred at -78°C for 2 h and a 5 mL THF solution of SiCl_4 (0.742 g, 4.36 mmol) was added dropwise through syringe. The reaction mixture was first kept stirring at -78°C for 1 h and then warmed up to room temperature and stirred overnight. The reaction mixture was extracted by ethyl ether followed by washing with DI H_2O and saturated brine solution. After the organic layer was dried with anhydrous Na_2SO_4 , the solvent was removed by rotor-vapor. The crude product was then purified by silica gel chromatography with hexanes to yield **11** as a white powder (2.24 g, 78.9%). ^1H NMR (300.13 MHz, CDCl_3): δ (10^{-6}) = 7.33 (Ph-H, d, 8H, $J_{\text{HH}}^3 = 8.4 \text{ Hz}$), 7.53 (Ph-H, d, 8H, $J_{\text{HH}}^3 = 8.1 \text{ Hz}$). ^{13}C NMR (75.48 MHz, CDCl_3): δ (10^{-6}) = 125.4, 131.4, 131.5, 137.6.

5-Bromothiophene-2-carbaldehyde (2) 2-Bromothiophene (21.6 mL, 0.223 mol) was injected via syringe into a 1 L 3-neck round bottom flask equipped with an addition funnel and a stir bar under positive N_2 pressure. Anhydrous THF (ca. 400 mL) was transferred into the flask through cannular. Lithium diisopropylamide solution (2 mol/L in THF/heptane/ethylbenzene, 123.0 mL, 0.246 mol) was transferred into the addition funnel and added dropwise at -78°C . The reaction mixture was kept stirring at -78°C for 30 min and then warmed up to room temperature. Anhydrous N,N -dimethylformamide (25.8 mL, 0.335 mol) was added slowly through a degassed syringe. The reaction mixture was further stirred at room temperature overnight. After standard aqueous workup, compound **1** was obtained as a colorless liquid by vacuum distillation. (37.0 g, 86.8%). ^1H NMR (300.13 MHz, CDCl_3): δ (10^{-6}) = 7.19 (Th-H, d, 1H, $J_{\text{HH}}^3 = 4.1 \text{ Hz}$), 7.52 (Th-H, d, 1H, $J_{\text{HH}}^3 = 4.1 \text{ Hz}$), 9.78 (-CHO, s, 1H).

5"-Bromo-3"-hexyl-(2,2':5',2"-terthiophene)-5-carbaldehyde (8) Compound **7** (1.092 g, 4.00 mmol) and compound **5** (1.588 g, 4.80 mmol) were dissolved in 30 mL anhydrous DMF in a pressure vessel containing a magnetic stir bar inside an argon filled glove box. $\text{Pd}(\text{PPh}_3)_4$ (69.3 mg, 1.5 mol%) was then added to the reaction mixture. The pressure vessel was sealed and taken out of the glove box. The reaction was carried out at 80°C for 24 h and then cooled to room temperature. After standard aqueous workup, compound **8** was further purified by silica gel chromatography with hexane/ethyl acetate (1.28 g, 88.9%). ^1H NMR (300.13 MHz, CDCl_3): δ (10^{-6}) = 0.89 (- CH_3 , t, 3H, $J_{\text{HH}}^3 = 6.9 \text{ Hz}$), 1.28-1.41 (- CH_2 -, m, 6H), 1.65 (- CH_2 -, m, 2H), 2.78 (- CH_2 -, t, 2H, $J_{\text{HH}}^3 = 7.8 \text{ Hz}$), 6.96 (Th-H, d, 1H, $J_{\text{HH}}^3 = 6.6 \text{ Hz}$), 7.07 (Th-H, d, 1H, $J_{\text{HH}}^3 = 3.6 \text{ Hz}$), 7.22 (Th-H, d, 1H, $J_{\text{HH}}^3 = 4.8 \text{ Hz}$), 7.25 (Th-H, d, 1H, $J_{\text{HH}}^3 = 4.2 \text{ Hz}$), 7.32 (Th-H, d, 1H, $J_{\text{HH}}^3 = 3.6 \text{ Hz}$), 7.68 (Th-H, d, 1H, $J_{\text{HH}}^3 = 3.9 \text{ Hz}$), 9.87 (-CHO, s, 1H). ^{13}C NMR (75.48 MHz, CDCl_3): δ (10^{-6}) = 13.9, 22.4, 29.0, 29.1, 30.2, 31.4, 123.6, 124.2, 126.2, 126.3, 129.5, 130.0, 134.9, 137.1, 138.0, 140.1, 141.2, 146.5, 182.0.

5"-Bromo-3"-hexyl-(2,2':5',2"-terthiophene)-5-(1,3-dioxolane) (9) Compound **8** (1.28 g, 3.55 mmol), ethyleneglycol (2.0 mL, 35.8 mmol) and a catalytic amount of *p*-toluenesulfonic acid were dis-

solved in 50 mL benzene in a 100 mL round bottom flask equipped with a Dean-Stark apparatus. The reaction mixture was refluxed at 150 °C for 24 h. The resulted reaction mixture was extracted by ethyl ether and followed by washing with saturated NaHCO₃, DI H₂O and saturated brine solution. After the organic layer was dried with anhydrous Na₂SO₄, the solvent was removed by rotor-vapor. The crude compound was further dried under vacuum and used for next step without further purification (1.24 g, 86.4%). ¹H NMR (300.13 MHz, CDCl₃) δ (10⁻⁶) = 0.88 (–CH₃, t, 3H, J_{HH}³ = 6.6 Hz), 1.26–1.39 (–CH₂–, m, 6H), 1.64 (–CH₂–, m, 2H), 2.76 (–CH₂–, t, 2H, J_{HH}³ = 7.8 Hz), 4.04 (–OCH₂–, m, 2H), 4.14 (–OCH₂–, m, 2H), 6.09 (–OCHO–, s, 1H), 6.93 (Th–H, d, 1H, J_{HH}³ = 5.1 Hz), 7.01 (Th–H, d, 1H, J_{HH}³ = 3.6 Hz), 7.05 (Th–H, d, 1H, J_{HH}³ = 3.6 Hz), 7.07 (Th–H, d, 1H, J_{HH}³ = 3.6 Hz), 7.11 (Th–H, d, 1H, J_{HH}³ = 3.6 Hz), 7.17 (Th–H, d, 1H, J_{HH}³ = 5.1 Hz). ¹³C NMR (75.48 MHz, CDCl₃) δ (10⁻⁶) = 14.1, 22.6, 29.2, 29.3, 30.6, 31.6, 65.2, 100.2, 123.0, 123.9, 124.2, 126.4, 127.0, 130.1, 130.2, 135.6, 136.8, 138.2, 139.9, 140.6.

3''-Hexyl-5''-trimethylstannyl-(2,2':5',2''-terthiophene)-5-(1,3-dioxolane) (10) Compound **9** (0.505 g, 1.25 mmol) was weighed into a dry 100 mL Schlenk flask under nitrogen, and 50 mL anhydrous THF was transferred through a cannular. The flask was cooled to –78 °C and 0.55 mL n-BuLi (2.5 mol/L in THF, 1.37 mmol) solution was added dropwise through a degassed syringe. The reaction mixture was stirred at –78 °C for 30 min and warmed up to room temperature. A Me₃SnCl solution (1 mol/L in THF, 1.5 mL, 1.5 mmol) was then added dropwise. The reaction mixture was kept stirring at room temperature overnight. The resulting reaction mixture was extracted by ethyl ether, followed by washing with DI H₂O and saturated brine solution. After the organic layer was dried with anhydrous Na₂SO₄, the solvent was removed by rotor-vapor. The crude compound was further dried under high vacuum and used for next step without further purification (0.709 g, 100%). ¹H NMR (300.13 MHz, CDCl₃) δ (10⁻⁶) = 0.38 (–CH₃, s, 9H), 0.87 (–CH₃, t, 3H, J_{HH}³ = 6.9 Hz), 1.26–1.39 (–CH₂–, m, 6H), 1.64 (–CH₂–, m, 2H), 2.78 (–CH₂–, t, 2H, J_{HH}³ = 7.8 Hz), 4.02 (–OCH₂–, m, 2H), 4.15 (–OCH₂–, m, 2H), 6.08 (–OCHO–, s, 1H), 6.99 (Th–H, d, 1H, J_{HH}³ = 3.9 Hz), 7.00 (Th–H, s, 1H), 7.04 (Th–H, d, 1H, J_{HH}³ = 3.6 Hz), 7.06 (Th–H, d, 1H, J_{HH}³ = 3.9 Hz), 7.10 (Th–H, d, 1H, J_{HH}³ = 3.6 Hz). ¹³C NMR (75.48 MHz, CDCl₃) δ (10⁻⁶) = –8.2, 14.1, 22.6, 29.2, 29.3, 30.7, 31.6, 65.2, 100.2, 122.9, 124.2, 126.0, 127.0, 135.9, 136.0, 136.5, 136.8, 138.3, 138.4, 140.4, 141.0.

Compound 11 Compound **1** (0.170 g, 0.26 mmol), compound **10** (0.709 g, 1.25 mmol) and Pd (PPh₃)₄ (9 mg, 3 mol%) were dissolved in 20 mL anhydrous DMF in a pressure vessel containing a magnetic stir bar under argon. The pressure vessel was sealed and stirred at 90 °C for 24 h. After cooling to room temperature, the reaction mixture was extracted with CHCl₃, followed by washing with 1 mol/L HCl, saturated NaHCO₃, DI H₂O and brine. After the organic layer was dried with anhydrous Na₂SO₄, the solvent was removed by rotor-vapor. The crude product was further purified by silica gel chromatography with dichloromethane/ethyl acetate to yield **12** as a brown solid (200 mg, 43.3%). ¹H NMR (300.13 MHz, CDCl₃) δ (10⁻⁶) = 0.90 (–CH₃, t, 12H, J_{HH}³ = 6.9 Hz), 1.32–1.43 (–CH₂–, m, 24H), 1.71 (–CH₂–, m, 8H), 2.81 (–CH₂–, t, 8H, J_{HH}³ = 4.8 Hz), 7.13 (Th–H, d, 4H, J_{HH}³ = 3.6 Hz), 7.24 (Th–H, s, 4H), 7.27 (Th–H, d, 4H, J_{HH}³ = 3.6 Hz), 7.33 (Th–H, d, 4H, J_{HH}³ = 3.9 Hz), 7.64 (Ph–H, m, 16H), 7.68 (Th–H, d, 4H, J_{HH}³ = 3.9 Hz), 9.87 (–CHO, s, 4H). ¹³C NMR (75.48 MHz, CDCl₃) δ (10⁻⁶) = 14.1, 22.6, 29.2, 29.7, 30.4, 31.6, 124.0, 125.0, 126.5, 126.6, 126.8, 129.9, 133.1, 135.1, 135.3, 136.9, 137.4, 138.1, 141.5, 141.6, 142.2, 146.8, 182.4. TOF MS (APPI⁺): Calcd. for SiC₁₀₀H₉₂O₄S₁₂N: 1768.3414 [M⁺], 1791.3312 [M + Na⁺]; found: 1768.3419 [M⁺], 1791.3317 [M + Na⁺].

n-Octyl cyanoacetate (12) Cyanoacetic acid (5.00 g 58.8 mmol), octanol (9.8 mL 61.8 mmol) and a catalytic amount of p-toluenesulfonic acid were dissolved in 30 mL benzene into a 100 mL round bottom flask equipped with a Dean-Stark apparatus. The reaction mixture was refluxed at 120 °C for 24 hours. After solvent removal under vacuum, **13** was purified by vacuum distillation as a colorless liquid (9.40 g 81.1%). ¹H NMR (300.13 MHz, CDCl₃): δ (10⁻⁶) = 0.89 (–CH₃, t, 3H, J_{HH}³ = 6.9 Hz), 1.28–1.38 (–CH₂–, m, 10H), 1.68 (–CH₂–, m, 2H), 3.45 (–CH₂–, s, 1H), 4.20 (–OCH₂–, t, 2H, J_{HH}³ = 6.9 Hz). ¹³C NMR (75.48 MHz, CDCl₃): δ (10⁻⁶) = 14.0, 22.6, 24.7, 25.7, 28.3, 29.1, 31.7, 67.1, 113.0, 162.9.

SO Compound **11** (88 mg 0.05 mmol), compound **12** (98.5 mg 0.50 mmol) and 1 mL triethylamine were dissolved in 30 mL CHCl₃. The reaction mixture was purged with N₂ for 30 min and then stirred at room temperature for 48 h. After solvent removal under vacuum, **SO** was purified by silica gel chromatography with hexane/dichloromethane and then precipitation into methanol as a dark red solid (105 mg 84.5%). ¹H NMR (300.13 MHz, CDCl₃): δ (10⁻⁶) = 0.89–0.90 (–CH₃, t, 24H), 1.31–1.34 (–CH₂–, m, 64H), 1.69–1.77 (–CH₂–, m, 16H), 2.82 (–CH₂–, t, 8H, J_{HH}³ = 7.8 Hz), 4.29 (–OCH₂–, t, 8H, J_{HH}³ = 6.9 Hz), 7.14 (Th–H, d, 4H, J_{HH}³ = 3.9 Hz), 7.25 (Th–H, d, 4H, J_{HH}³ = 3.9 Hz), 7.27 (Th–H, s, 4H), 7.37 (Th–H, d, 4H, J_{HH}³ = 3.9 Hz), 7.64 (Ph–H, m, 16H), 7.67 (Th–H, d, 4H, J_{HH}³ = 4.2 Hz), 8.26 (–CH=C, s, 4H). ¹³C NMR (75.48 MHz, CDCl₃): δ (10⁻⁶) = 14.1, 22.6, 25.8, 28.6, 29.2, 29.7, 30.4, 31.7, 31.8, 66.6, 97.7, 116.0, 124.2, 125.0, 126.7, 126.8, 126.9, 129.9, 133.2, 134.3, 135.0, 136.9, 138.6, 139.1, 141.7, 142.4, 146.1, 147.1, 163.0.

5 Acknowledgment

The authors would like to acknowledge University of New Mexico for financial support for this research. National Science Foundation (NSF) is acknowledged for supporting the NMR facility at UNM through grants CHE-0840523 and 0946690.

References:

- [1] HOPPE H, SARICIFTCI N S. Organic solar cells: An overview [J]. J Mater Res 2004, 19(7):1924–1945.
- [2] SPANGGAARD H, KREBS F C. A brief history of the development of organic and polymeric photovoltaics [J]. Sol Energy Mater Sol Cells 2004, 83(2–3):125–146.
- [3] THOMPSON B C, FRECHET J M. Polymer – fullerene composite solar cells [J]. Angew Chem Int Ed 2008, 47(1):58–77.
- [4] DENNLER G, SCHARBER M C, BRABEC C. Polymer – fullerene bulk-heterojunction solar cells [J]. Adv Mater 2009, 21(13):1323–1338.
- [5] CHENGY J, YANG S H, HSU C S. Synthesis of conjugated polymers for organic solar cell applications [J]. Chem Rev, 2009, 109(11):5868–5923.
- [6] HE Z, ZHONG C, SU S, et al. Enhanced power-conversion efficiency in polymer solar cells using an inverted device structure [J]. Nat Photon 2012, 6:591–595.
- [7] YOU J, DOU L, YOSHIMURA K, et al. A polymer tandem solar cell with 10.6% power conversion efficiency [J]. Nat Commun 2013, 4, doi:10.1036/n Comms 2411.
- [8] YOU J, CHEN C C, HONG Z, et al. 10.2% power conversion efficiency polymer tandem solar cells consisting of two identical sub-cells [J]. Adv Mater 2013, 25(29):3973–3978.
- [9] MISHRA A, BAUERLE P. Small molecule organic semiconductors on the move: promises for future solar energy technology

- [J]. *Angew Chem Int Ed* 2012, 51(9):2020–2067.
- [10] WALKER B, KIM C, NGUYEN T Q. Small molecule solution-processed bulk heterojunction solar cells [J]. *Chem Mater*, 2011, 23(3):470–482.
- [11] CHEN Y, WAN X, LONG G. High performance photovoltaic applications using solution-processed small molecules [J]. *Acc Chem Res* 2013, 46(11):2645–2655.
- [12] STEINMANN V, KRONENBERG N M, LENZE M R et al. Simple, highly efficient vacuum-processed bulk heterojunction solar cells based on merocyanine dyes [J]. *Adv Energy Mater* 2011, 1(5):888–893.
- [13] SUN Y, WELCH G C, LEONG W et al. Solution-processed small-molecule solar cells with 6.7% efficiency [J]. *Nat Mater* 2012, 11:44–48.
- [14] LIU X, SUN Y, PEREZ L A et al. Narrow-band-gap conjugated Chromophores with Extended Molecular Lengths [J]. *J Am Chem Soc* 2012, 134(51):20609–20612.
- [15] ROQUET S, DE B R, LERICHE P et al. Three-dimensional tetra(oligothienyl) silanes as donor material for organic solar cells [J]. *J Mater Chem* 2006, 16:3040–3045.
- [16] LIN Z, BJORGAARD J, YAVUZ A G et al. Low band gap star-shaped molecules based on benzothia(oxa)diazole for organic photovoltaics [J]. *J Phys Chem C* 2011, 115:15097–15108.
- [17] PU S, ZHENG C, SUN Q et al. Enhancement of cyclization quantum yields of perfluorodiarylethenes via weak intramolecular interactions [J]. *Chem Commun* 2013, 49:8036–8038.
- [18] GRISORIO R, DE M L, ALLEGRETTA G et al. Anchoring stability and photovoltaic properties of new D(– π –A)₂ dyes for dye-sensitized solar cell applications [J]. *Dyes Pigments* 2013, 98(2):221–231.
- [19] AMIR E, SIVANANDAN K, COCHRAN J E et al. Synthesis and characterization of soluble low-bandgap oligothiophene–[all]–S,S-dioxides-based conjugated oligomers and polymers [J]. *J Polym Sci A Polym Chem*, 2011, 49(9):1933–1941.
- [20] CROUCH D J, SPARROWE D, HEENEY M et al. Polyterthiophenes Incorporating 3,4-Difluorothiophene Units: Application in Organic Field-Effect Transistors [J]. *J Macromol Chem Phys* 2010, 211(24):2642–2648.

一种三维四面体星型共轭小分子用于有机太阳能电池

秦 洋, 阳建中

(美国新墨西哥大学 化学和化学生物系 新墨西哥州 阿尔伯克基 87131–0001)

摘 要: 合成了一种由四苯基硅烷为中心和氰基脂功能化三联噻吩为支链构成的新型三维四面体星型小分子 SO。循环伏安曲线测得这种小分子拥有很低的 HOMO 能级(–5.3 eV)和较窄的能带(1.9 eV)。吸收光谱、X 射线散射和差示扫描量热法实验都显示这种化合物拥有很高的结晶度。制作和测试了基于 SO 分子的太阳能电池。光学显微镜实验证实相对低的光电转化效率主要是由于没有形成很好的相分离。

关键词: 四面体星型小分子; 有机太阳能电池; 结晶度; 相分离

(责任编辑: 郁 慧)